Journal of Medicinal Chemistry



# Analyses of synthetic N-Acyl Dopamine derivatives reveal differential structural requirements for their anti-inflammatory and transient receptor potential channel of the vanilloid receptor subfamily subtype 1 (TRPV1) activating properties

Prama Pallavi, Marc Pretze, Julio Caballero, Yingchun Li, Björn B. Hofmann, Eleni Stamellou, Sarah Klotz, Carmen Wängler, Björn Wängler, Ralf Loesel, Steffen Roth, Bastian Theisinger, Handan Moerz, Uta Binzen, Wolfgang Greffrath, Rolf-Detlef Treede, Martin C. Harmsen, Bernhard K. Krämer, Mathias Hafner, Benito A. Yard, and Anna-Isabelle Kälsch

*J. Med. Chem.*, **Just Accepted Manuscript** • DOI: 10.1021/acs.jmedchem.8b00156 • Publication Date (Web): 15 Mar 2018



ACS Publications

is published by the American Chemical Society. 1155 Sixteenth Street N.W., Washington, DC 20036

| | |
|---|---|
| | Krämer, Bernhard; Medizinische Fakultät Mannheim der Universität Heidelberg, V. Department of Medicine<br>Hafner, Mathias; Hochschule Mannheim, Institute for Molecular and Cellular Biology<br>Yard, Benito; Medizinische Fakultät Mannheim der Universität Heidelberg, V. Department of Medicine<br>Kälsch, Anna-Isabelle; Medizinische Fakultät Mannheim der Universität Heidelberg, V. Department of Medicine |
| | |

# Analyses of synthetic *N*-Acyl Dopamine derivatives reveal differential structural requirements for their anti-inflammatory and transient receptor potential channel of the vanilloid receptor subfamily subtype 1 (TRPV1) activating properties

*Prama Pallavi[1,2], Marc Pretze[3], Julio Caballero[4], Yingchun Li[1], Björn B. Hofmann[1], Eleni Stamellou[1], Sarah Klotz[1], Carmen Wängler[5], Björn Wängler[3], Ralf Loesel[6], Steffen Roth[6], Bastian Theisinger[7], Handan Moerz[8], Uta Binzen[8], Wolfgang Greffrath[8], Rolf-Detlef Treede[8], Martin C. Harmsen[9], Bernhard K. Krämer[1], Mathias Hafner[2], Benito A. Yard[1*], Anna-Isabelle Kälsch[1]*

[1] V Department of Medicine, University Hospital Mannheim, Medical Faculty Mannheim, Heidelberg University, Mannheim 68167, Germany; [2] Institute for Molecular and Cellular Biology, Mannheim University of Applied Sciences, Mannheim 68163, Germany; [3] Molecular Imaging and Radiochemistry, Department of Clinical Radiology and Nuclear Medicine Medical Faculty Mannheim of Heidelberg University, Mannheim 68167, Germany; [4] Center for Bioinformatics and Molecular Simulations, Faculty of Engineering in Bioinformatics, Universidad de Talca, Talca 3460000, Chile; [5] Biomedical Chemistry, Department of Clinical Radiology and Nuclear Medicine, Medical Faculty Mannheim of Heidelberg University,Mannheim 68167, Germany; [6] Department of Applied Chemistry, Technical University of Applied Sciences, Nuremberg 90489, Germany; [7] CeloNova BioSciences Germany

GmbH, Heidelberg 69120, Germany; [8] Division of Neurophysiology, Centre of Biomedicine and Medical Technology Mannheim (CBTM), Medical Faculty Mannheim, Heidelberg University, Mannheim 68167, Germany; [9] University of Groningen, University Medical Centre Groningen, Department of Pathology and Medical Biology, Groningen 9713, The Netherlands.

**Abstract**

We studied the chemical entities within *N*-octanoyl dopamine (NOD) responsible for transient receptor potential channels of the vanilloid receptor subtype 1 (TRPV1) activation and inhibition of inflammation. The potency of NOD to activate TRPV1 was significantly higher compared to variants in which the ortho-dihydroxy groups were acetylated, one of the hydroxy groups was omitted (*N*-octanoyl tyramine) or the ester functionality consisted of a bulky fatty acid (*N*-pivaloyl dopamine). Shortening of the amide linker (ΔNOD) slightly increased its potency which further increased by interchanging the carbonyl and amide groups (ΔNODR). With the exception of ΔNOD, the presence of an intact catechol structure was obligatory for inhibition of VCAM-1 and induction of HO-1 expression. Since TRPV1 activation and inhibition of inflammation by *N*-acyl dopamines require different structural entities, our findings provide a framework for the rational design of TRPV1 agonists with improved anti-inflammatory properties.

## Introduction

*N*-acyl dopamines (NADs) are condensation products of fatty acids linked to dopamine at the amino group. They show agonistic properties at the transient receptor potential channel of the vanilloid receptor subfamily subtype 1 (TRPV1), are capable of activating the cannabinoid receptors CB1 and CB2 and show anti-inflammatory and immune modulatory effects[1-4]. TRPV1 is mainly expressed in unmyelinated C- and thinly myelinated Aδ-afferent nerve fibers[5, 6] and significantly contributes to the generation of pain signals, i.e. nociception. It is essential for selective modalities of pain sensation, e.g. tissue injury-induced thermal hyperalgesia [7] as observed in the course of inflammation [8], incision-induced postoperative pain [9], visceral nociception [10] or neuropathic pain conditions [11, 12].

There is growing evidence that supports a prominent role for inflammation in the development and maintenance of neuropathic pain. TRPV1 activation by NADs has been reported to modulate nociceptive signaling in inflammatory pain[13-15]. Independent hereof, NADs also exhibit anti-inflammatory properties on their own through inhibition of transcription factors involved in inflammation, e.g. NFκB, NFAT and AP-1 [1, 2]. We have previously demonstrated that *N*-octanoyl dopamine (NOD), a synthetic NAD, strongly inhibits Tumor necrosis factor alpha (TNFα) mediated vascular cell adhesion molecule-1 (VCAM-1) expression along with a variety of inflammatory chemo- and cytokines [16]. Moreover, like other catechol containing structures NOD induces the expression of heme oxygenase-1 (HO-1), as a consequence of Nrf-2 activation[17]. These properties make NOD an interesting molecule to ameliorate tissue damage, either caused by inflammation or oxidative stress as inciting events. Indeed we have shown that NOD has a salutatory effect on ischemia induced acute kidney injury (AKI) in rats [18] and that its use in brain dead donor rats improves renal function in recipient rats[19].

Analogous to capsaicin (CAP), an archetypic TRPV1 agonist, NADs can be structurally divided into three parts, i.e. the aromatic moiety (A-region), the linker region containing the amide bond (B-region) and the hydrophobic aliphatic side chain (C-region)[20-22]. NOD differs from CAP in structure as it contains a catechol instead of a vanilloid moiety (the A-region), is one methylene group longer (the B-region) and contains a completely saturated aliphatic chain (the C-region) (Figure 1A).

In this study we try to asses what structural moieties impart NADs TRPV1 agonistic properties and what structural moieties impart its anti-inflammatory properties. We used NOD as a lead compound and subsequently made changes in the A-, B- and C-region to delineate to what extent this affects TRPV1 activation and its anti-inflammatory properties in terms of inhibiting TNFα mediated VCAM-1 and HO-1 induction.

## Results

*Generation of structural derivatives of NOD*

To assess the moieties within NOD that are required for TRPV1 activation, we used NOD as a lead structure. We synthesized compounds that differ from NOD at the aromatic moiety (A-region), the linker region (B-region) or the aliphatic chain (C-region). These changes included acetylation of the catechol structure, (A-NOD), removal of one hydroxyl functional group from the benzene nucleus (*N*-octanoyl tyramine (NOT)), exchanging octanoyl for the branched pivaloyl as aliphatic chain (*N*-pivaloyl dopamine (NPiD)), and shortening of the linker region by one methylene group. The latter was made in two variants in which the positions of the carbonyl group were interchanged relative to the position of the amide group (ΔNOD and ΔNODR) (Figure 1B). In addition the vanilloid moiety of CAP was changed to a catechol structure (CAP-

OH) (Figure 1C). We chose a different way for synthesis of CAP-OH as Goto et al [23]. Natural capsaicin was reduced and yielded saturated and unsaturated compounds with and without $CH_3O$-group. Only purification via semi-preparative HPLC led to the pure CAP-OH.

*NOD derivatives have differential TRPV1 activation properties*

TRPV1 activation by the synthetic NADs was assessed using calcium microfluorimetry on rTRPV1 transfected HEK293 cells. Neither the synthetic NADs nor CAP induced change of intracellular calcium concentrations ($[Ca^{++}]_i$) in untransfected HEK293 cells (Supplementary Figure S1).

Even though NOD dose dependently increased $[Ca^{++}]_i$ in rTRPV1 transfected HEK293 cells (Figure 2A), it was significantly less potent and effective as compared to CAP (Figure 2 B) NOD $EC_{50}$ 5.93 µM versus CAP $EC_{50}$ 0.87 µM (Table 1). Two-way ANOVA (fixed effects) indicated significant effects of concentration ($F_{(7,86)} = 39.96$, $p < 0.001$), of substance ($F_{(1,86)} = 216.04$, $p < 0.001$) as well as significant interactions ($F_{(7,86)} = 9.38$, $p < 0.001$; see Fig. 2A for LSD post-hoc tests).

The application of 30µM NOD led to a significant increase in $[Ca^{++}]_i$ ($p < 0.03$) compared to vehicle control, and these cells also responded to the specific TRPV1 agonist capsaicin CAP. With repetitive NOD application, calcium influx displayed marked tachyphylaxis and decreased to 60 ± 6.3 % from the first to the fifth response (Figure 2C-D; $p<0.001$) a typical response feature known from activation of TRPV1 by CAP. Application of TRPV1 antagonist capsazepine (CPZ) 30 sec before the second NOD stimulus, significantly reduced responses (to 78 ± 3.4 % of 1st versus 35 ± 5.1 % of 1st without/with CPZ $p<0.001$) further supporting that NOD is an agonist at TRPV1. Interestingly, under these conditions NOD-evoked responses were persistently

reduced after wash-out of CPZ, while capsaicin CAP responsiveness of these cells was not changed indicating that, however, those differences are preasumably not fully explained by an incomplete washed-out of the lipophilic compound by an aqueous buffer solution (Figure 2 C and D; $p = 0.89$).

All synthetic NOD derivatives were able to activate TRPV1 in a concentration-dependent manner (Figure 3; NOD, ΔNOD, ΔNODR ($F_{(7,132)} = 38.69$, $p < 0.001$); NOD, A-NOD ($F_{(4,63)} = 9.39$, $p < 0.001$). ΔNODR was the most potent while and A-NOD was the least potent (3-fold reduction) and efficacious (2 fold reduction) in comparison to NOD (ANOD $EC_{50} = 18.69$ μM, efficacy 1.06 ± 0.19 vs NOD $EC_{50} = 5.93$μM, efficacy 2.34±0.08). Although ΔNOD showed improved potency and efficacy ΔNODR was the most potent (ΔNOD $EC_{50} = 3.69$μM, efficacy 4.39 ± 0.32 ΔNODR $EC_{50} = 0.07$μM efficacy 3.14±0.22) (Table 1). Two-way ANOVA indicated significant effects of substance (NOD, ΔNOD, ΔNODR ($F_{(2,132)} = 20.72$, $p < 0.001$ and NOD, A-NOD $F_{(1,63)} = 9.01$, $p < 0.01$) as well as significant interactions for NOD, ΔNOD, ΔNODR ($F_{(14,132)} = 3.04$, $p < 0.001$) but not for NOD, A-NOD ($F_{(4,63)} = 1.39$, $p > 0.2$).

CAP-OH also activated TRPV1 in a dose dependent manner ($F_{(9,87)} = 82.94$, $p < 0.001$). Although it retained agonistic properties at TRPV1 CAP-OH displayed an $EC_{50}$ value of 4.93 μM, much higher than that of CAP $EC_{50}$ 0.87 μM (Table 1). However, two-way ANOVA failed to indicate overall significant effects between CAP and CAP-OH ($F_{(1,87)} = 0.04$, $p > 0.8$; interaction term $F_{(9,87)} = 1.62$, $p > 0.12$) (Supplementary figure S2).

Because NOT and NPiD precipitated at high concentrations (1 mM) at which calcium transients were only 38 % and 51 % of the CAP response, $EC_{50}$ values could not be determined. It should

be mentioned however that slight calcium transients for NOT and NPiD were observed at 100 and 500 μM respectively.

*NOD, CAP and the NOD derivatives use similar amino acids for their TRPV1 interaction*

Based on the electron cryo-microscopy structure of the rTRPV1 ion channel [24], we performed docking studies with NOD, CAP, and the NOD derivatives to understand the interaction between the agonist and the channel. We observed potential hydrogen bond interactions for CAP with three amino acids Y511, T550 and E570 (Figure 4A) in the TRPV1 binding pocket. For NOD, two of these interactions were the same, i.e. T550 and E570, while no hydrogen bond interaction with Y511 was suggested (Figure 4B).

The NOD derivatives established hydrogen bond interactions with the same residues (Figure 4D-H), with the exception of A-NOD, which is oriented differently because the lack of OH substituents in its catechol group (Figure 4C). The hydrogen bond distances obtained from the docking positions of the studied compounds (without considering A-NOD) are shown in the Supplementary Table S1. It is possible to observe that NOD, CAP, and the NOD derivatives form one or two hydrogen bond interactions with the residue E570. Meanwhile, all the compounds, with the exception of NPiD, form a hydrogen bond with T550. Finally, the compounds CAP, ΔNODR, NPiD and CAP-OH are hydrogen bonded to Y511.

The docking method Glide XP yielded a scoring energy value for each compound reported in Figure 4. Despite docking methods are not so reliable in calculating binding energy values,[25] a good correlation between the Glide XP scoring energy values and experimental $\log EC_{50}$ values was found with correlation coefficient $R^2 = 0.66$ (Figure 4I). This result confirms that the selected electron cryo-microscopy structure is a good model for studying the affinities of TRPV1 ligands, and gives confidence in the ability of the Glide XP method to describe the relationship

between the chemical interactions of the ligands in the binding site and their differential affinities. It is possible to extract per-residue coulombic, hydrogen bond, and van der Waals (VDW) components from the Glide XP scoring energy to get more insight in the most relevant TRPV1 amino acids involved in the differential activities (Supplementary Figure S3). The analysis of the coulombic components indicates that E570 has the major contribution, which is better when both catechol hydroxyl groups are available. The analysis of the hydrogen bond components shows that the residues Y511, T550 and E570 have different energy contributions for each compound. Finally, the analysis of the VDW contributions is more complex due to multiple residues involved. The residues with higher VDW contributions were Y511, L515, F522, F543, A546, M547, T550, N551, L553, Y554, I569, and I573 from chain A, and F587, F591, I661, L662, A665, and L669 from chain B. It is noteworthy to mention that Y511 has not only a hydrogen bond contribution; it also has an important VDW contribution. This chemical role was suggested previously in the report of Lee et al.[26]: when the Y511F and Y511A mutants were generated, capsaicin $EC_{50}$ values increased 30 times for the first mutant (where hydrogen bond contribution was lost and VDW contribution was kept), and 500 times for the second (where both hydrogen bond and VDW contributions were lost).

To evaluate the interactions revealed by the docking model and previously published anchor residues S512 and R491[27] for the CAP TRPV1 interactions, all putative interacting amino acids in rTRPV1 were changed to alanine by site-directed mutagenesis. The effect of these mutations on TRPV1 activation was studied at three different concentrations of CAP (300 nM, 1 μM, and 10 μM; Figure 5A) and NOD (15 μM, 50 μM and 200 μM; Figure 5B) corresponding to approximately 2.5, 9 and 36 (for NOD) or 1, 3 and 30 (for CAP) times the $EC_{50}$ value. For the Y511A and E570A rTRPV1 variants the calcium responses were completely lost at the two lower concentrations of CAP or NOD and remained significantly diminished even when using

excessively high concentrations of CAP or NOD (Figure 5 A-B). Also the T550A significantly diminished TRPV1 activation, which seemed to be more pronounced in the case of NOD stimulation at 15 μM (two times $EC_{50}$) and at 200 μM (three times $EC_{50}$). While in HEK cells expressing the S512A TRPV1 variant CAP was not able to evoke calcium responses when tested over a range of concentration (Supplementary figure S4), mutation of R491 to A did not affect TRPV1 activation by CAP or NOD.

*The anti-inflammatory property of NADs is not defined solely by Redox activity*

To assess if the structural changes in the synthetic compounds would also affect their anti-inflammatory properties, we screened all the compounds for down-regulation of TNFα mediated VCAM-1 expression and induction of HO-1 in HUVECs (Figure 6A). Except for ΔNOD all catechol containing structures were able to inhibit TNFα mediated VCAM-1 expression, while this was neither observed for CAP nor for NOT. Inhibition of VCAM-1 expression was paralleled by a concomitant induction of HO-1 expression. Dose-response experiments for direct comparison of NOD vs NOT, CAP vs CAP-OH and ΔNOD vs. ΔNODR are depicted in figure 6 B-D. In considering that catechols contain a high redox activity which may contribute to the anti-inflammatory effects of NADs[16], we assessed for each compound except for Capsaicin the quenching properties in a peroxidase mediated luminol chemiluminescence reaction (Table 1). Enzymatic oxidation of the capsaicin leads to formation of dimer which might interfere with the measurement of luminescence[28] therefore redox activity of Capsaicin was not measured. All compounds except for NOT were able to quench chemiluminescence in the luminol assay at a similar strength.

## Discussion

We previously demonstrated that apart from TRPV1 activation, NOD exerts profound cyto-protective properties including prevention of cold inflicted injury [29-31], down-regulation of inflammatory mediators [16] and inhibition of platelet function[31]. In the present study we dissected the moieties within NOD that govern TRPV1 activation and are responsible for the anti-inflammatory effect as defined by down-regulation of TNFα mediated VCAM-1 expression and induction of HO-1. The major findings of this study are as follows: firstly, NOD is an agonist at rTRPV1 in a HEK293 heterologous expression system but activates TRPV1 with lesser potency than CAP. Alterations in the A-, B- and C-regions of NOD may all affect the potency and efficacy to stimulate TRPV1. While shortening of the linker region by one methylene group improved the ability of NADs to activate TRPV1(NOD $EC_{50}$ = 5.93μM, ΔNOD $EC_{50}$ = 3.69μM, ΔNODR $EC_{50}$ = 0.07μM) the use of a short branched fatty acid in the C-region (NPiD) or omission of a hydroxyl group in the A region (NOT) profoundly deteriorated TRPV1 activation. Acetylation of both hydroxyl groups in the A-region (A-NOD) impaired TRPV1 activation to a much lesser extent. Secondly, docking studies suggested that amino acids (AA) Y511, E570 and T550 in TRPV1 may form hydrogen bond interactions with CAP, while only E570 and T550 form this interaction with NOD. In addition to these putative interacting AA, site directed mutagenesis also revealed the importance of S512 for TRPV1 activation by CAP or NOD. Thirdly, the anti-inflammatory effects of the compounds were not significantly affected by changes in the A-, B- and C-regions of NOD as long as the catechol moiety in the A-region was maintained. Acetylation of the ortho-dihydroxy groups (A-NOD) was equally effective as compared to NOD. Moreover attainment of catechol structure imparted CAP-OH better anti-inflammatory property as compared to CAP. The only exception found in this study was ΔNOD

which did not inhibit VCAM-1 expression despite the fact that it carries an intact catechol structure.

The CAP-bound TRPV1 structure was recently resolved by making use of cryo-EM[24, 32] and iterative computation in conjunction to systematic site-specific functional tests[33]. From these data it has been postulated that CAP takes a 'tail-up, head-down' configuration in which the vanillyl and amide groups form specific interactions with residues T550 and E570 by hydrogen bonds to anchor to its bound position. The aliphatic chain interacts with the channel through nonspecific VDW forces and contributes to the binding affinity. This is followed by a series of structural rearrangements to stabilize the activated conformation mainly by 'pulling' at E570 through hydrogen bonding and VDW forces. The Y511 residue seems not to play a role in hydrogen binding but closes the mouth of the binding pocket and thereby cradling the CAP molecule inside[33]. This model thus explains why the Y511A mutation leads to impaired TRPV1 activation, but does address the importance of S512 for TRPV1 activation by CAP [27] and NOD. Although S512 is not directly present in the binding pocket, it might contribute to the shape of the binding pocket and thus might be indirectly required for attaining the appropriate binding pocket configuration for the interaction with TRPV1 agonists. This might explain why we did not achieve TRPV1 activation by any of the TRPV1 agonist in cells expressing the S512A TRPV1 mutant. Our docking studies suggest similar interactions for NOD and TRPV1 as described for CAP, i.e. interaction of the catechol group with E570 and interaction of the amide with T550.

Acetylation of both hydroxyl groups in the A-region (A-NOD) yielded loss of TRPV1 activation potency and significantly lower 340/380-ratio for A-NOD as compared to NOD. It should be emphasized that our docking studies suggest that A-NOD would not fit in the TRPV1 pocket

unless it is converted to NOD via intracellular esterases. This might as well explain why the 340/380-ratio was lower for A-NOD. Both NPiD and NOT were extremely poor TRPV1 agonists. According to docking experiments, the former does not fit in the hydrophobic region of the TRPV1 pocket because of the short bulky fatty acid tail or the short bulky fatty acid tail does not provide sufficient VDW forces in the interaction with the hydrophobic core of the channel[33]. On the other hand, NOT enters in the TRPV1 pocket but only allows one hydrogen bond with E570, as opposed to two bonds for NOD. This results in a relative loss of binding affinity and thus in impaired TRPV1 activation. Shortening of the linker region on the contrary, increased the potency of NADs to activate TRPV1 (ΔNOD $EC_{50}$ = 2.87 μM and ΔNODR $EC_{50}$ = 0.06 μM). In fact, ΔNODR was even more potent than CAP ($EC_{50}$=0.305 μM) in activating TRPV1. Although our TRPV1 docking model didn't predict any difference between ΔNODR and CAP with respect to the total energy value, the coulombic and hydrogen bond contributions of E570 and the hydrogen bond contribution of Y511 are suggested as the more important chemical characteristics for explaining ΔNODR's lower $EC_{50}$ value.

ΔNOD and ΔNODR also behaved differently with respect to the anti-inflammatory properties. These properties seem to depend on the presence of the catechol structure which acts as an anti-oxidant able to inhibit NFκB [16] and to activate the Nrf2-keap1 pathway[17]. In line with this, it was found that CAP-OH is more superior to CAP in inhibiting VCAM-1 and inducing HO-1 expression. Yet, despite having an intact catechol structure and high redox activity ΔNOD completely failed to inhibit TNFα mediated VCAM-1 and to induce HO-1. This underlines that redox activity alone is not determining anti-inflammatory property.

## Conclusions

In conclusion, it was demonstrated that the moieties that govern TRPV1 activation by NOD, and presumably NADs in general, are different from the ones that provide NADs their anti-inflammatory properties. As TRPV1 is a ubiquitous receptor that is involved in the processing of noxious stimuli and inflammation,our findings may thus provide a framework for the rational design of moderate TRPV1 agonists with improved anti-inflammatory properties for the treatment of inflammatory pain.

## Experimental section

### General procedures

*Chemicals*

All chemical reagents were purchased from Sigma Aldrich (Sigma-Aldrich Chemie GmbH, Munich, Germany) unless otherwise indicated.

### Site directed mutagenesis

A pcDNA3-rTRPV1 construct was used to generate rTRPV1-R491A (5'-gca gga aat att gaa tcc ctg cga aga aga agt aga ctc ctc-3'; 5'-gag gag tct act tct tct tcg cag gga ttc aat att tcc tgc-3); T511A (5'-gta caa aga aaa gta tct cac tgg cgc tgt cca caa aca aac tct tga-3', 5'-tca aga gtt tgt ttg tgg aca gcg cca gtg aga tac ttt tct ttg tac-3'); S512A (5'ctg tac aaa gaa aag tat ctc ata ggc gct gtc cac aaa caa act-3', 5'-gag ttt gtt tgt gga cag cgc cta tga gat act ttt ctt tgt aca-3'); T550A (5'-gta gag cat gtt ggc cca gcc cat ggc ca-3', 5'-tgg cca tgg gct ggg cca aca tgc tct ac-3'); and E570A (5'-ctg tac aaa gaa aag tat ctc agc gta gct gtc cac aaa caa act c-3', 5'-gag ttt gtt tgt gga cag cta cgc tga gat act ttt ctt tgt aca g-3') mutations using QuikChange Site-Directed Mutagenesis Kit (Agilent Technologies) as per manufactures' protocol. Sequence of all the clones was verified by using BigDye® Terminator v3.1 Cycle Sequencing Kit at the Department of Pathology by Dr. Christian Saur.

**Cell culture**

HEK293 cells (obtained from ATCC, LGC Standards, Teddington, UK) were cultured in T25cm$^2$ flasks with Dulbecco's modified Eagle's medium (DMEM; PAA, Pasching, Austria) supplemented with 10 % fetal calf serum (FCS Gold, ;PAA), 100 U/l penicillin and 100 µg/mL streptomycin (PAA) at 37°C in a 5 % $CO_2$ humidified atmosphere. 24 h prior to transfection, 4.0 x $10^5$ cells per well were plated on poly-L-lysine (10 µg/mL) coated round (Ø 15 mm) coverslips, transfected with 1 µg pcDNA3-rTRPV1 or the mutated constructs using 3 µL Metafectene (metafectene® pro - Biontex Laboratories GmbH) and incubated at 34°C in a 5 % $CO_2$ humidified atmosphere.

Human umbilical vein endothelial cells (HUVECs) were isolated from the freshly available umbilical cord. Cells were grown in basal endothelial cell growth medium (Provitro GmbH, Berlin Germany), supplemented with 2 % fetal bovine serum, without antibiotics at 37ºC in a 5 % $CO_2$ humidified atmosphere and experiments were conducted at approximately 80-90 % visual confluence.

**Calcium Imaging**

48 h post transfection cells were transferred into extracellular solution containing NaCl 137.6 mM, KCl 5.4 mM, $MgCl_2$ 0.5 mM, $CaCl_2$ 1.8 mM, glucose 5 mM and HEPES 10 mM (Roth, Karlsruhe, Germany), loaded with the fluorescent dye FURA-2AM (3 µM; Biotrend, Köln, Germany) and 3 µM Pluronic F-127 for 45 min at RT in dark. Followed by 20 min washout in extracellular solution, fluorescence was measured using an inverted microscope (IX-81 with Cell^R, Olympus, Hamburg, Germany) and an ORCA-R2 CCD camera (Hamamatsu Corp., Bridgewater, NJ, USA). After alternating excitation with light of 340 nm and 380 nm wavelength, the ratio of the fluorescence emission intensities at 510 nm (340nm/380nm [510nm]) was digitized at 0.5 Hertz and calculated. This fluorescence ratio is a relative measure of

intracellular calcium concentration[34]. The concentration range at which calcium transients appeared upon stimulation with each of the compounds was established by application of increasing concentration of compounds for 1 min in a single coverslip of rTRPV1 transfected HEK293 cells followed by a washout for 1 min (inter-stimulus interval: 5 min). For $EC_{50}$ determination a minimum of nine concentrations of each compound based on this range were used. Only one concentration per coverslip and a minimum of three separate coverslips for each concentration was used. The compound was applied to the cells for 1 min followed by 1 min washout using perfusion and 2 min rest. Repetitive application of 30 μM NOD was used to investigate tachyphylaxis. Additionally, 30 s before the second stimulus vehicle or 30 μM of the competitive TRPV1 antagonist Capsazepine was applied to block the receptor. At the end of each experiment 10 μM CAP was used to select transfected cells and only cells responding to this suprathreshold stimulus were included in analysis. Ionomycin (10 μM) was occasionally applied at experiments' end[35] responses to 10 μM capsaicin and to ionomycin were highly correlated in the same cells ($r = 0.89$, $p < 0.001$; $n = 38$). Analysis was done using cell^R software (Olympus). Each coverslip was considered as an independent experiment. Absolute change in ratio was determined by subtracting baseline value from the peak.

**Protein isolation and Western Blotting**

HUVECs were lysed in 20 mM Tris-HCl, 150 mM NaCl, 5 mM EDTA, 1% Triton X-100, 0.5% sodium deoxycholate, 1 μM dithiothreitol (DTT) buffer containing proteinase and phosphatase inhibitors. Protein concentrations were measured using Coomassie-Reagent (Pierce, Rockford, USA). 15 μg of protein per condition was loaded on 10 % SDS-polyacrylamide gel. Human anti-VCAM-1 (1:2000, BBA19, R&D Systems, Germany) or Human anti-HO-1 (1:2000, ADI-SPA-896-F, Enzo, Biochem Inc.) antibodies were used to probe the membrane. Since these compounds do not influence expression of β-Actin, equal protein loading was confirmed by stripping and re-

probing membranes with monoclonal human anti-β-actin antibody (1:10,000, Abcam plc, UK). Anti-goat IgG-HRP, anti-rabbit IgG-HRP, anti-mouse IgG-HRP conjugated secondary antibodies (1:2500, Santa Cruz Biotechnology) were used. Image J ver1.5e was used for densitometry analysis. All the lanes were normalized to β-Actin. Inhibition of VCAM-1 is expressed as percentage relative to that of TNFα; induction of HO-1 is expressed as fold increase relative to that of cells grown in normal culture medium.

**Luminol Assay**

The redox activity of the compounds was measured using luminol assay. Serial dilutions of the compounds were prepared in distilled water, added to the luminol reaction mix (luminol 2.5 mM, p-Coumaric acid 0.9 mM and 0.3 % $H_2O_2$). HRP (0.1 µg/µL) and quenching of chemiluminescence was measured immediately using infinite® 200 PRO – Tecan microplate reader. The measurements were performed in triplicates.

**Molecular modeling**

Because of structural similarity between NOD and CAP the structure of TRPV1 PDB 3J5R[24], in which the TRPV1 forming complex with CAP is modelled, was taken. This structure is a reconstruction of the above mentioned complex by single particle cryo-microscopy[32]. The protein structure was processed with the Protein Preparation Wizard in the Schrödinger Suite 2005 (Maestro, Version 9.0, 2007; Schrödinger, LLC: New York, NY, USA), two chains are needed for delimiting the binding site, denoted as chain A and B in the manuscript. Hydrogen atoms were added followed by the adjustment of bond orders. The protonation states for protonable residues were adjusted to match pH = 7.4. After this, the protein was subjected to geometry optimization by using OPLS_2005 force field[36]. The structures of the different NADs were sketched by using the chemical editor at Maestro and were prepared using LigPrep (two-

dimensional representations were converted into three-dimensional ones and partial charges were assigned).

Glide software was used for performing docking analyses[37]. The grid box for molecular docking was centered in the middle of the pocket, close to Y511, including the amino acids of chain A and B present in the binding site. The extra precision (XP) Glide mode was used. Glide XP has empirical scoring functions and also imposes desolvation penalties for burial of protein or ligand polar and charged groups. The method adds explicit water molecules to poses selected in previous steps, counts them, and uses these counts for performing comparisons with analogous groups in known active compounds. This process reduces false positives and increases reliability of the docking energy values. In our approach, the best docked position for each complex was determined by considering the total energy value after five runs.

**Statistical analysis**

All data are expressed as the means ± SEM from at least three independent experiments. Statistical significance of results was assessed by one- or two-way ANOVA followed by LSD Statistica 4.5 for Windows, StatSoft Inc., $p<0.05$ was considered to be significant. For comparison, data were normalized to the respective first response. Prism 6 for Windows Version 6.was used for preparation of the figures.

**Materials.**

**General procedures.** All reagents and solvents were purchased from commercial suppliers and were used without further purification unless otherwise specified. NMR spectra were recorded on a 250 MHz Bruker AC250, a 300 MHz Varian Mercury Plus and a 500 MHz Varian NMR System spectrometer (Palo Alto, CA). Chemical shifts ($\delta$) are given in ppm and are referenced to the residual solvent resonance signals relative to $(CH_3)_4Si$ ($^1H$, $^{13}C$). Mass spectra were obtained

on a Bruker Daltonics microflex™ MALDI-TOF mass spectrometer (Bremen, Germany). Preparative column chromatography was performed on Merck silica gel 60. Reactions were monitored by thin-layer chromatography (TLC) on Merck silica gel F254 aluminum plates, with visualization under UV (λ = 254 nm). If necessary, the purity was determined by high performance liquid chromatography (HPLC). Purity of all final compounds was 95% or higher (Supplementary Table S2). HPLC was performed on a Dionex UltiMate 3000 HPLC system (Thermo Scientific, Dreieich, Germany), equipped with a reverse phase column (Merck Chromolith RP-18e; analytical: 100x4.6 mm plus a guard column 10x4.6mm; semipreparative: 100x10 mm plus a guard column 10x10 mm) and a UV-diode array detector (210 nm, 254 nm). The solvent system used was a gradient of acetonitrile:water (containing 0.1% TFA) (0–8 min: 0–100% MeCN) at a flow rate of 4 mL/min unless otherwise stated.

**N-acyl dopamine synthesis.** *N*-octanoyl dopamine (NOD) (**1**), *N*-pivloyl dopamine (NPiD) (**2**) and *N*-octanoyl tyramine (NOT) (**3**) were prepared from commercially available precursors as described previously [30]. The compounds were purified by two fold recrystallization from dichloromethane, and purity of the compounds was confirmed by HPLC. Briefly, octanoic acid was converted to its mixed anhydride derivative by reaction with ethyl chloroformate in the presence of *N*-ethyl diisopropylamine. The crude mixed anhydride was incubated with dopamine hydrochloride in *N,N*-dimethylformamide and *N*-ethyl diisopropylamine to form NOD. After aqueous preparation and evaporation of the organic solvent NOD is obtained in an overall yield of 60 %. The sample investigated by NMR (Bruker AC250) yielded spectra in accordance with the expected structure.

*N-(3,4-dihydroxyphenethyl)pivalamide (NPiD) (**2**).* Analytical HPLC: $t_R$ = 1.50 min (>97%). $^1$H NMR (250 MHz, $CDCl_3$): $\delta$ = 8.69 (s, 2H, 2xOH), 7.46 (t, $^3J$ = 6.6 Hz, 1H, NH), 6.62 (d, $^3J_{H5,H6}$ = 7.9 Hz, 1H, H-5), 6.55 (dd, $^3J_{H5,H6}$ = 7.9 Hz, $^4J_{H2,H6}$ = 1.9 Hz, 1H, H-6), 6.41 (d, $^4J_{H2,H6}$

= 1.9 Hz, 1H, H-2), 3.14 (dt, $^3J_{H,H}$ = 7.4 Hz, $^3J_{NH,H}$ = 6.6 Hz, 2H, $NCH_2$), 2.50 (d, $^3J$ = 7.4 Hz, 2H, $BnCH_2$), 1.07–1.04 ppm (m, 9H, 3x$CH_3$).

*4-(2-Octanamidoethyl)-1,2-phenylene diacetate (A-NOD) (**4**).* Acetylation of NOD was performed by suspending **1** (2 g, 7.16 mmol) of in acetic anhydride (5 mL) under magnetic stirring. When two drops of sulphuric acid were added, the suspension turned clear and stirring was continued for one hour. Diluted hydrochloric acid (5 mL) was added and 30 min later the reaction mixture was poured into 200 mL ice water. The precipitated product was collected by vacuum filtration and dried under vacuum to yield pure A-NOD, confirmed by HPLC. Analytical HPLC: $t_R$ = 3.38 min (>97%). $^1$H NMR (250 MHz, $CDCl_3$): $\delta$ = 7.12 (d, $^3J_{H5,H6}$ = 8.1 Hz, 1H, H-5), 7.06 (dd, $^3J_{H5,H6}$ = 8.1 Hz, $^4J_{H2,H6}$ = 2.0 Hz, 1H, H-6), 7.01 (d, $^4J_{H2,H6}$ = 2.0 Hz, 1H, H-2), 3.49 (dt, $^3J_{H,H}$ = 7.5 Hz, $^3J_{NH,H}$ = 6.7 Hz, 2H, $NCH_2$), 2.81 (d, $^3J$ = 7.5 Hz, 2H, $BnCH_2$), 2.89 (s, 6H, 2x$AcCH_3$), 2.13 (t, $^3J$ = 7.7 Hz, 2H, H-α), 1.63–1.56 (m, 2H, H-β), 1.33–1.19 (m, 8H, H-γ,δ,ε,ζ), 0.89–0.86 ppm (m, 3H, $CH_3$).

*N-(3,4-Dihydroxybenzyl)octanamide (ΔNOD) (**5**).* To a stirring solution of 3,4-dihydroxybenzylamine hydrobromide (300 mg, 1.36 mmol) and $NaHCO_3$ (377 mg, 4.49 mmol) in $H_2O$ (5 mL), $CHCl_3$ was added after 30 min and after 15 min a fresh solution of octanoyl chloride (232 µL, 1.36 mmol) in $CHCl_3$ (1 mL) was added and the solution was stirred at 40°C for 18 h. Water was added (10 mL) and the solution was extracted 3x with $CHCl_3$ (10 mL). The organic phase was washed with 0.5 M HCl (10 mL) and brine (10 mL) and dried with $MgSO_4$. The $CHCl_3$ was removed and the crude product was purified by semi preparative HPLC (0–75% MeCN in $H_2O$ + 0.1 TFA within 6 min at 4 mL/min). The fractions containing the product were collected and lyophilized to give **5** as colorless powder (66 mg, 34%). $R_F$ = 0.36 (EA:CH 2:1). $^1$H NMR (300 MHz, $CDCl_3$): $\delta$ = 6.87 (d, $^4J_{H2,H6}$ = 2.0 Hz, 1H, H-2), 6.80 (d, $^3J_{H5,H6}$ = 8.1 Hz, 1H, H-5), 6.62 (dd, $^3J_{H5,H6}$ = 8.1 Hz, $^4J_{H2,H6}$ = 2.0 Hz, 1H, H-6), 4.31 (d, $^3J$ = 8.1 Hz, 2H, $BnCH_2$),

2.23 (t, $^{3}J$ = 7.7 Hz, 2H, H-α), 1.67–1.57 (m, 2H, H-β), 1.27–1.22 (m, 8H, H-γ,δ,ε,ζ), 0.87–0.85 ppm (m, 3H, $CH_3$). $^{13}$C NMR (75 MHz, $CDCl_3$): $\delta$ = 174.3 (C=O), 144.5 (C-3), 144.1 (C-4), 130.1 (C-1), 119.9 (C-6), 116.9 (C-2), 114.8 (C-5), 43.5 ($BnCH_2$), 36.7 (C-α), 31.6 (C-ε), 29.1 (C-γ), 28.9 (C-δ), 25.8 (C-β), 22.6 (C-ζ), 14.0 ppm ($CH_3$). MS (MALDI-TOF): *m/z* (%) 266 (100) $[M + H]^+$. Analytical HPLC: $t_R$ = 2.69 min (>96%). See supplementary figure S5 for NMR signal assignment.

*2-(3,4-Dihydroxyphenyl)-N-octylacetamide (ΔNODR) (**6**).* (Compound **4g** from Walpole et al.[38], no NMR data) To a solution of 3,4-dihydroxyphenylacetic acid (300 mg, 1.78 mmol) in dry THF (8 mL) under an argon atmosphere, $Et_3N$ (249 µL, 1.78 mmol) and ethyl chloroformate (165 µL, 1.78 mmol) were added and stirred 3 h in the dark at ambient temperature. Then octylamine (296 µL, 1.78 mmol) was added and the solution was stirred for 18 h. To the solution was added EA and the organic phase was washed with brine and dried with $MgSO_4$. The solvent was removed and the crude product was purified by column chromatography (CH → CH:EA 4:1 → 1:1) to obtain the product **6** as colorless solid (138 mg, 28%). $R_F$ = 0.24 (EA:CH 1:1). $^{1}$H NMR (500 MHz, $CDCl_3$): $\delta$ = 6.83 (d, $^{3}J_{H5,H6}$ = 8.1 Hz, 1H, H-5), 6.75 (d, $^{4}J_{H2,H6}$ = 1.7 Hz, 1H, H-2), 6.48 (dd, $^{3}J_{H5,H6}$ = 8.1 Hz, $^{4}J_{H2,H6}$ = 1.7 Hz, 1H, H-6), 3.40 (s, 2H, $BnCH_2$), 3.24 (dd, $^{3}J_{H,H}$ = 13.5 Hz, $^{3}J_{NH,H}$ = 6.7 Hz, 2H, H-α), 1.52–1.46 (m, 2H, H-β), 1.28–1.22 (m, 10H, H-γ,δ,ε,ζ,η), 0.87–0.84 ppm (m, 3H, $CH_3$). $^{13}$C NMR (126 MHz, $CDCl_3$): $\delta$ = 175.2 (C=O), 144.7 (C-3), 144.3 (C-4), 124.3 (C-1), 121.2 (C-6), 116.5 (C-5), 115.9 (C-2), 41.2 ($BnCH_2$), 40.7 (C-α), 31.7 (C-ζ), 29.1 (C-ε), 29.0 (C-δ), 28.6 (C-β), 26.8 (C-γ), 22.6 (C-η), 14.1 ppm ($CH_3$). MS (MALDI-TOF): *m/z* (%) 279 (100) $[M + H]^+$. Analytical HPLC: $t_R$ = 3.12 min (>98%).

*(E)-N-(3,4-dihydroxybenzyl)-8-methylnon-6-enamide (CAP-OH) (**7**).* (Compound **1** from Goto et al. [23], no NMR data) To a solution of natural Capsaicin (162 mg, 0.53 mmol) and $K_2CO_3$ (220 mg, 1.59 mmol) in $CH_2Cl_2$ (30 mL), a 1 M solution of $BBr_3$ in $CH_2Cl_2$ (1.32 mL) was

slowly added at -18°C within 5 min and the mixture was stirred for 60 min to reach -16°C. Water (20 mL) was added for quenching them reaction and the mixture was extracted with $CH_2Cl_2$ (1x) and EA (1x). The combined organic phases were washed with brine (20 mL) and dried with $MgSO_4$. The solvent was removed and the crude product was purified by column chromatography (CH → CH:EA 4:1 → 2:1 → 1:1) to obtain a yellow oil (117 mg, 76%). The yellow oil was further purified by semi preparative HPLC (0–50% MeCN in $H_2O$ + 0.1 TFA within 8 min at 4 mL/min). The fractions containing the product were collected and lyophilized to give **7** as colorless powder (45 mg, 29%). $R_F$ = 0.33 (EA:CH 2:1). $^1$H NMR (500 MHz, $CDCl_3$): $\delta$ = 6.85 (s, 1H, H-5), 6.79 (s, 1H, H-2), 6.60 (d, $^3J_{H5,H6}$ = 8.0 Hz, 1H, H-6), 5.37–5.25 (m, 2H, HC=CH), 4.29 (s, 2H, $BnCH_2$), 2.26 (t, $^3J$ = 7.6 Hz, 2H, H-α), 1.95 (dd, $^3J$ = 13.9 Hz, $^4J$ = 7.0 Hz, 1H, CH), 1.67–1.59 (m, 2H, H-δ), 1.38–1.23 (m, 4H, H-β,γ), 0.94 (s, 3H, $CH_3$), 0.93 ppm (s, 3H, $CH_3$). $^{13}$C NMR (126 MHz, $CDCl_3$): $\delta$ = 174.6 (C=O), 144.4 (C-3), 144.1 (C-4), 138.5 (C-ζ), 129.7 (C-1), 126.2 (C-ε), 119.9 (C-6), 115.0 (C-5), 114.9 (C-2), 43.7 (BnC), 36.4 (C-α), 32.1 (C-δ), 30.9 (C-η), 29.1 (C-γ), 25.3 (C-β), 22.6 ppm (2x$CH_3$). MS (MALDI-TOF): *m/z* (%) 292 (100) $[M + H]^+$. Analytical HPLC: $t_R$ = 3.08 min (>95%).

## Ancillary Information

**Ethical Statement :** Umbilical cords for isolation of human umbilical vein endothelial cells (HUVECs) were received from donors in the Department of Obstetrics and Gynecology, University Medical Center Mannheim, Heidelberg University, Mannheim, Germany. This was approved by the local ethics committee (Medizinische Ethikkommission II der Medizinischen Fakultät Mannheim) and all donors gave their written informed consent (Ethics Application No. 2015-518N-MA).

**Supporting Information:** The Supporting Information is available- Molecular formula Strings of the compounds, immunofluorescence method protocol, $[Ca^{++}]_i$ response in nontransfected HEK293 cells, per-residue docking chemical components from Glide XP scoring energies for the studied compounds, $[Ca^{++}]_i$ response experiments showing S512A mutation in rTRPV1 leads to loss of TRPV1 activation by Capsaicin, NMR assignment, Hydrogen bond distances (Å) to the residues Y511, T550, and E570 for the studied compounds from docking obtained poses and HPLC retention time and purity of compounds.

**Corresponding Author Information:**

Prof. Benito A. Yard, V. Medical Clinic, University Hospital Mannheim, Theodor-Kutzer-Ufer 1-3, D-68167 Mannheim, Germany, Tel: 0049-621-383 3212, Fax: 0049-621-383 3804, E-mail: benito.yard@medma.uni-heidelberg.de

**Author Contribution** : PP, ES, JC, MP, SR ,BH, YL, HM and BT performed the experiments. PP, JC, MP, BAY, CW, RL, WG UB BKK and AIK analyzed the results. PP, WG, UB, BAY, MH and SK were involved in the design of the study. PP, BW, WG, UB, MCH, BKK, MH, RDT, BAY, and AIK wrote the paper.

**Disclosure :**

All other submitting authors declare that they do not have any conflict of interest with this publication.

**Acknowledgement:** We would like to thank Prof. Dr. Hans-Günter Schmalz and Dr. Nikolay Sitnikov from Department of Chemistry, University of Cologne, for their invaluable discussion

on the chemical structures and findings of this study We like to acknowledge Dr. Christian Saur, from Department of Pathology, University Hospital Mannheim, for his help with the sequencing of the mutants. This study was supported by grants from the Deutsche Forschungsgemeinschaft (GRK880/3) and Albert und Anneliese Konanz-Stiftung.

**Abbreviations Used :** NAD *N*-acyl dopamine; NOD N-octanoyl dopamine; ANOD acetylated NOD; TRPV1 transient receptor potential channels of the vanilloid receptor subtype 1; NOT *N*-octanoyl tyramine; NPiD *N*-pivaloyl dopamine; TNF-α Tumor necrosis factor alpha; VCAM-1 Vascular cell adhesion protein 1; HO-1 Heme oxygenase-1; CB Cannabinoid receptors; NFκB Nuclear factor κB; NFAT Nuclear factor of activated T-cells; AP-1 Activator protein 1; AKI acute kidney injury; CAP Capsaicin, VDW Van der Waals; CPZ Capsazepine

**References:**

1. Navarrete, C. M.; Perez, M.; de Vinuesa, A. G.; Collado, J. A.; Fiebich, B. L.; Calzado, M. A.; Munoz, E. Endogenous N-acyl-dopamines induce COX-2 expression in brain endothelial cells by stabilizing mRNA through a p38 dependent pathway. Biochemical pharmacology **2010,** *79*, 1805-1814.

2. Sancho, R.; Macho, A.; de La Vega, L.; Calzado, M. A.; Fiebich, B. L.; Appendino, G.; Munoz, E. Immunosuppressive activity of endovanilloids: N-arachidonoyl-dopamine inhibits activation of the NF-kappa B, NFAT, and activator protein 1 signaling pathways. Journal of immunology **2004**, *172*, 2341-2351.

3. Chu, C. J.; Huang, S. M.; De Petrocellis, L.; Bisogno, T.; Ewing, S. A.; Miller, J. D.; Zipkin, R. E.; Daddario, N.; Appendino, G.; Di Marzo, V.; Walker, J. M. N-oleoyldopamine, a

novel endogenous capsaicin-like lipid that produces hyperalgesia. The journal of biological chemistry **2003**, *278*, 13633-13639.

4. Bisogno, T.; Melck, D.; Bobrov, M.; Gretskaya, N. M.; Bezuglov, V. V.; De Petrocellis, L.; Di Marzo, V. N-acyl-dopamines: novel synthetic CB(1) cannabinoid-receptor ligands and inhibitors of anandamide inactivation with cannabimimetic activity in vitro and in vivo. The biochemical journal **2000**, *351 Pt 3*, 817-824.

5. Kaufman, M. P.; Iwamoto, G. A.; Longhurst, J. C.; Mitchell, J. H. Effects of capsaicin and bradykinin on afferent fibers with ending in skeletal muscle. Circulation research **1982**, *50*, 133-139.

6. Belmonte, C.; Gallar, J.; Pozo, M. A.; Rebollo, I. Excitation by irritant chemical substances of sensory afferent units in the cat's cornea. The journal of physiology **1991**, *437*, 709-725.

7. Caterina, M. J.; Leffler, A.; Malmberg, A. B.; Martin, W. J.; Trafton, J.; Petersen-Zeitz, K. R.; Koltzenburg, M.; Basbaum, A. I.; Julius, D. Impaired nociception and pain sensation in mice lacking the capsaicin receptor. Science **2000**, *288*, 306-313.

8. Fischer, M. J.; Btesh, J.; McNaughton, P. A. Disrupting sensitization of transient receptor potential vanilloid subtype 1 inhibits inflammatory hyperalgesia. The Journal of neuroscience : the official journal of the Society for Neuroscience **2013**, *33*, 7407-7414.

9. Pogatzki-Zahn, E. M.; Shimizu, I.; Caterina, M.; Raja, S. N. Heat hyperalgesia after incision requires TRPV1 and is distinct from pure inflammatory pain. Pain **2005**, *115*, 296-307.

10. Cervero, F.; Laird, J. M. Understanding the signaling and transmission of visceral nociceptive events. Journal of neurobiology **2004**, *61*, 45-54.

11. Baron, R. Neuropathic pain: a clinical perspective. Handbook of experimental pharmacology 2009, 3-30.

12. Butera, J. A. Current and emerging targets to treat neuropathic pain. Journal of medicinal chemistry **2007**, *50*, 2543-2546.

13. Spicarova, D.; Palecek, J. The role of the TRPV1 endogenous agonist N-Oleoyldopamine in modulation of nociceptive signaling at the spinal cord level. Journal of neurophysiology **2009**, *102*, 234-243.

14. Farkas, I.; Tuboly, G.; Benedek, G.; Horvath, G. The antinociceptive potency of N-arachidonoyl-dopamine (NADA) and its interaction with endomorphin-1 at the spinal level. Pharmacology, biochemistry, and behavior **2011**, *99*, 731-737.

15. De Petrocellis, L.; Chu, C. J.; Moriello, A. S.; Kellner, J. C.; Walker, J. M.; Di Marzo, V. Actions of two naturally occurring saturated N-acyldopamines on transient receptor potential vanilloid 1 (TRPV1) channels. British journal of pharmacology **2004**, *143* , 251-256.

16. Hottenrott, M. C.; Wedel, J.; Gaertner, S.; Stamellou, E.; Kraaij, T.; Mandel, L.; Loesel, R.; Sticht, C.; Hoeger, S.; Ait-Hsiko, L.; Schedel, A.; Hafner, M.; Yard, B.; Tsagogiorgas, C. N-octanoyl dopamine inhibits the expression of a subset of kappaB regulated genes: potential role of p65 Ser276 phosphorylation. PloS one **2013**, *8*, e73122, https://doi.org/10.1371/journal.pone.0073122.

17. Kim, H.; Kim, W.; Yum, S.; Hong, S.; Oh, J. E.; Lee, J. W.; Kwak, M. K.; Park, E. J.; Na, D. H.; Jung, Y. Caffeic acid phenethyl ester activation of Nrf2 pathway is enhanced under oxidative state: structural analysis and potential as a pathologically targeted therapeutic agent in treatment of colonic inflammation. Free radical biology & medicine **2013**, *65*, 552-562.

18. Tsagogiorgas, C.; Wedel, J.; Hottenrott, M.; Schneider, M. O.; Binzen, U.; Greffrath, W.; Treede, R. D.; Theisinger, B.; Theisinger, S.; Waldherr, R.; Kramer, B. K.; Thiel, M.; Schnuelle, P.; Yard, B. A.; Hoeger, S. N-octanoyl-dopamine is an agonist at the capsaicin receptor TRPV1

and mitigates ischemia-induced [corrected] acute kidney injury in rat. PloS one **2012**, *7*, e43525, https://doi.org/10.1371/journal.pone.0043525.

19. Spindler, R. S.; Schnuelle, P.; Nickels, L.; Jarczyk, J.; Waldherr, R.; Theisinger, S.; Theisinger, B.; Klotz, S.; Tsagogiorgas, C.; Gottmann, U.; Kramer, B. K.; Yard, B. A.; Hoeger, S. N-Octanoyl Dopamine for Donor Treatment in a Brain-death Model of Kidney and Heart Transplantation. Transplantation **2015**, *99*, 935-941.

20. Walpole, C. S.; Wrigglesworth, R.; Bevan, S.; Campbell, E. A.; Dray, A.; James, I. F.; Perkins, M. N.; Reid, D. J.; Winter, J. Analogues of capsaicin with agonist activity as novel analgesic agents; structure-activity studies. 1. The aromatic "A-region". Journal of medicinal chemistry **1993**, *36*, 2362-2372.

21. Walpole, C. S.; Wrigglesworth, R.; Bevan, S.; Campbell, E. A.; Dray, A.; James, I. F.; Masdin, K. J.; Perkins, M. N.; Winter, J. Analogues of capsaicin with agonist activity as novel analgesic agents; structure-activity studies. 3. The hydrophobic side-chain "C-region". Journal of medicinal chemistry **1993**, *36*, 2381-2389.

22. Walpole, C. S.; Wrigglesworth, R.; Bevan, S.; Campbell, E. A.; Dray, A.; James, I. F.; Masdin, K. J.; Perkins, M. N.; Winter, J. Analogues of capsaicin with agonist activity as novel analgesic agents; structure-activity studies. 2. The amide bond "B-region". Journal of medicinal chemistry **1993**, *36*, 2373-2380.

23. Goto, M.; Mizuma, H.; Wada, Y.; Suzuki, M.; Watanabe, Y.; Onoe, H.; Doi, H. 11C-labeled Capsaicin and its in vivo molecular imaging in rats by positron emission tomography. Food Nutr. Sci. **2015**, *6*, 216-220.

24. Liao, M.; Cao, E.; Julius, D.; Cheng, Y. Structure of the TRPV1 ion channel determined by electron cryo-microscopy. Nature **2013**, *504*, 107-112.

25. Ramirez, D.; Caballero, J. Is it reliable to use common molecular docking methods for comparing the binding affinities of enantiomer pairs for their protein target? International journal of molecular sciences **2016**, *17*, 525-540, doi:10.3390/ijms17040525

26. Lee, J. H.; Lee, Y.; Ryu, H.; Kang, D. W.; Lee, J.; Lazar, J.; Pearce, L. V.; Pavlyukovets, V. A.; Blumberg, P. M.; Choi, S. Structural insights into transient receptor potential vanilloid type 1 (TRPV1) from homology modeling, flexible docking, and mutational studies. J Comput Aided Mol Des **2011**, *25*, 317-327.

27. Jordt, S. E.; Julius, D. Molecular basis for species-specific sensitivity to "hot" chili peppers. Cell **2002**, *108*, 421-430.

28. Boersch, A.; Callingham, B. A.; Lembeck, F.; Sharman, D. F. Enzymic oxidation of capsaicin. Biochemical pharmacology **1991**, *41*, 1863-1869.

29. Vettel, C.; Hottenrott, M. C.; Spindler, R.; Benck, U.; Schnuelle, P.; Tsagogiorgas, C.; Kraemer, B. K.; Hoeger, S.; El-Armouche, A.; Wieland, T.; Yard, B. A. Dopamine and lipophilic derivates protect cardiomyocytes against cold preservation injury. The journal of pharmacology and experimental therapeutics **2013**, *348(1)*:, 77-85.

30. Losel, R. M.; Schnetzke, U.; Brinkkoetter, P. T.; Song, H.; Beck, G.; Schnuelle, P.; Hoger, S.; Wehling, M.; Yard, B. A. N-octanoyl dopamine, a non-hemodyanic dopamine derivative, for cell protection during hypothermic organ preservation. PloS one **2010**, *5*, e9713, https://doi.org/10.1371/journal.pone.0009713.

31. Ait-Hsiko, L.; Kraaij, T.; Wedel, J.; Theisinger, B.; Theisinger, S.; Yard, B.; Bugert, P.; Schedel, A. N-octanoyl-dopamine is a potent inhibitor of platelet function. Platelets **2013**, *24,* 428-434.

32. Cao, E.; Liao, M.; Cheng, Y.; Julius, D. TRPV1 structures in distinct conformations reveal activation mechanisms. Nature **2013**, *504*, 113-118.

33. Yang, F.; Xiao, X.; Cheng, W.; Yang, W.; Yu, P.; Song, Z.; Yarov-Yarovoy, V.; Zheng, J. Structural mechanism underlying capsaicin binding and activation of the TRPV1 ion channel. Nature chemical biology **2015**, *11*, 518-524.

34. Grynkiewicz, G.; Poenie, M.; Tsien, R. Y. A new generation of $Ca^{2+}$ indicators with greatly improved fluorescence properties. The Journal of biological chemistry **1985**, *260*, 3440-3450.

35. Moriello, A. S.; De Petrocellis, L. Assay of TRPV1 Receptor Signaling. Methods in molecular biology **2016**, *1412*, 65-76.

36. Jorgensen, W. L.; Maxwell, D. S.; Tirado-Rives, J. Development and testing of the OPLS all-atom force field on conformational energetics and eroperties of organic liquids. Journal of the american chemical society **1996**, *118*, 11225-11236.

37. Friesner, R. A.; Murphy, R. B.; Repasky, M. P.; Frye, L. L.; Greenwood, J. R.; Halgren, T. A.; Sanschagrin, P. C.; Mainz, D. T. Extra precision glide: docking and scoring incorporating a model of hydrophobic enclosure for protein-ligand complexes. Journal of medicinal chemistry **2006**, *49*, 6177-6196.

38. Walpole, C. S. J.; Wrigglesworth, R.; Bevan, S.; Campbell, E. A.; Dray, A.; James, I. F.; Perkins, M. N.; Reid, D. J.; Winter, J. Analogues of Capsaicin with agonist activity as novel analgesic agents; Structure-activity studies. 1. The aromatic “A-region". Journal of medicinal chemistry. **1993**, *36*, 2362-2372.

| Compound | Modified region(s) with respect to NOD | TRPV1 activation | | | Anti-inflammatory properties at 100μM | | Redox activity |
|---|---|---|---|---|---|---|---|
| | | $EC_{50}$ [μM] | LOG $EC_{50}$ | TOP | VCAM-1 Relative inhibition | HO-1 induction (fold increase) | $EC_{50}$ Luminol Assay[μM] |
| Capsaicin | | 0.87 | -6.06±0.19 | 6.09±0.34 | 1.13±0.18 | 2.81±0.31 | Not measured |
| NOD | none | 5.93 | -5.23±0.08 | 2.34±0.08 | 0.40±0.05**** | 10.12±3.06**** | 9.15 |
| A-NOD | A | 18.69 | -4.73±0.25 | 1.06±0.19 | 0.53±0.08*** | 6.11±1.95* | 14.80 |
| ΔNOD | B | 3.69 | -5.43±0.21 | 4.39±0.32 | 0.79±0.07** | 3.66±0.72 | 6.78 |
| ΔNODR | B | 0.06 | -7.22±0.13 | 3.14±0.26 | 0.43±0.07**** | 6.98±1.49**** | 7.70 |
| NOT | A | >100 | >-4 | N.D | 0.76±0.07** | 1.44±0.52 | >1000 |
| NPiD | C | >500 | >-3.3 | N.D | 0.53±0.12*** | 5.93±1.55* | 10.44 |
| CAP-OH | | 4.93 | -5.31±0.25 | 7.81±0.66 | 0.46±0.11**** | 4.86±0.97* | 37.52 |

**Table 1: TRPV1 activation, anti-inflammatory, and redox properties of the compounds used in the study.** For TRPV1 activation and Luminol Assay – the $EC_{50}$ value defined as the concentration of the compound needed to evoke the response corresponding to the 50 % of the maximum produced by that compound. The increase in ratio was fitted in $y = \text{Bottom} + \frac{(\text{Top}-\text{bottom})}{(1+10^{(\text{LogEC50}-X)\times\text{Hillslope}}}$ equation to obtain $\text{LogEC}_{50}$ values. For TRPV1 activation assay- bottom

was constrained to 0 since the baseline was subtracted from the response. Top in the equation refers to the platue observed in the dose response experiments and provides the efficacy i.e. maximum strength of TRPV1 activation.The anti-inflammatory property of the compounds was assessed at 100μM via their ability inhibit TNFα induced VCAM-1 expression or induction of HO-1at protein level. Western blot data quantification was performed by densitometry. Inhibition of VCAM-1 is expressed as relative to that of TNFα (10ng/ml), induction of HO-1 is expressed as fold increase relative to that of cells grown in normal culture medium. For each experiment and for each quantification chemiluminescence signal was normalized using ß-actin. Statistical analysis was performed using a one way-ANOVA with Fisher's LSD test, VCAM-1 inhibition - TNFα versus treatment, HO-1 induction medium versus treatment (n.s. non-significant, * $p < 0.05$, ** $p < 0.01$, *** $p<0.001$***$p<0.0001$,****$p < 0.0001$).

**Legends to the figures**

**Figure 1: Chemical structures of the studied compounds.** (**A**) CAP and NOD are shown with schematic representation of the different regions (A, B and C regions are shown with the dotted line). (**B**) Chemical structure of compounds used in the study, the structural region in which they vary from NOD is mentioned on the left side of the structure. NOD variants were synthesized by modifying the A- , B- and C-region region relative to that of NOD. (**C**) CAP-OH was synthesized by changing A region of CAP.

**Figure 2: NOD like Capsaicin (CAP) activates rTRPV1 (A).** A representative experiment showing increases in free $[Ca^{++}]_i$ in rTRPV1 transfected cells in response to 1 nM, 100 nM and 10 μM of CAP and NOD. The ratio 340/380 at 510 nm – a measure proportional to free $[Ca^{++}]_i$ – is false color coded where warmer colors indicate increasing calcium values. **(B)** Dose response curves of CAP (filled) and NOD (open circles). rTRPV1 expressing HEK293 cells were stimulated once with each concentration with at least three different measurements per concentration. The results are expressed as average ratio 340/380 at 510 nm ± SEM of all measurements. The $EC_{50}$ value of CAP was about 0.87 μM and for NOD 5.93 μM (indicated as dotted lines). Two-way ANOVA indicates substance differences; ** $p < 0.01$ and *** and $p < 0.001$ LSD post-hoc test. **(C)** A series of representative experiments showing increases in free $[Ca^{++}]_i$ in rTRPV1 transfected cells in response to repetitive application of 30 μM NOD. The response displayed marked tachyphylaxis from stimulus to stimulus (black trace). Application of equimolar concentration of the competitive TRPV1 antagonist Capsazepine before and during the $2^{nd}$ stimulus (CPZ; grey trace) abolished the NOD response further confirming that NOD acts as a full agonist at TRPV1. The ratios 340/380 at 510 nm – a measure proportional to free $[Ca^{++}]_i$ – was averaged from three independent experiments per condition and are shown as mean±SEM

(depicted as dotted line) **(D)** Bar graph shows the maximum increases in free $[Ca^{++}]_i$ upon response to repetitive application of 30 μM NOD with or without equimolar concentration of CPZ; repeated application of NOD induced tachyphylaxis of subsequent responses, CPZ largely blocked NOD responses – both phenomena are also known for capsaicin at TRPV1. *** $p < 0.001$, LSD post-hoc test vehicle versus CPZ group; + $p < 0.05$, ++ $p < 0.01$, +++ $p < 0.001$ versus preceding application within treatment group.

**Figure 3**: **Dose response curves obtained with different NADs**. rTRPV1 transfected HEK293 cells were stimulated only once and for each concentration at least 3 different measurements were done. The results are expressed as average ratio 340/380 at 510 nm ± SEM of all measurements with $EC_{50}$ values (indicated as dotted lines) of 5.93 μM (NOD, open circles), 18.69 μM (A-NOD, grey circles), 3.69 μM (ΔNOD, filled circles) and 0.06 μM (ΔNOD R, triangles). $^{n.s.}$ $p > 0.2$, $^{++}$ $p < 0.01$, $^{+++}$ $p < 0.001$ ANOVA with LSD post-hoc test between substances.

**Figure 4: Docking of capsaicin, NOD, and NOD derivatives in TRPV1 channel**. Conformations of the studied compounds within the binding pocket of TRPV1 for CAP (A), NOD (B), A-NOD (C), NOT (D), ΔNOD (E), ΔNODR (F), NPiD (G), and CAP-OH (H). Chain A of the protein is represented in yellow, where amino acids with hydrogen bond contributions Y511, T550 and E570 are in stick representations. Chain B of the protein is represented in orange, where amino acids with VDW contributions are also in stick representations. Glide XP scoring energy values are at the top-left corner of each docking pose picture (A-H). Correlation between these values and experimental $\log EC_{50}$ values are in (I).

**Figure 5: Point mutation of the identified binding sites dramatically changes the TRPV1 channels sensitivity to capsaicin (CAP) and NOD.** HEK293 cells were transfected with different mutants of the rTRPV1 receptor. Cells were challenged with different concentrations of either capsaicin (300 nM, 1 µM, 10 µM; **A**) or NOD (15 µM, 50 µm, 200 µM; **B**). Y511A, and E570A are important for the binding of both capsaicin and NOD. Regarding T550A the effect is more pronounced after NOD application. A minimum of 3 independent experiments were done. Statistical analysis was performed using two way-ANOVA with Fisher's LSD test wild-type tested versus mutated rTRPV1 at the same concentration (n.s. non-significant, * $p < 0.05$, ** $p < 0.001$, ***$p<0.0001$).

**Figure 6: Anti-inflammatory property is not solely governed via catechol structure. (A)** HUVECs were stimulated overnight with - TNFα (10 ng/mL) in the presence of 100 µM various compounds. The expression of VCAM-1 and HO-1 was determined by western blotting and quantified by densitometry. VCAM-1 expression is presented as fold change relative to TNFα (T) and HO-1 expression is presented as fold change relative to medium (M) (**B**-**D**) Dose-response experiments for direct comparison of NOD vs NOT (**B**), Capsaicin (CAP) vs. CAP-OH (**C**) and ΔNOD vs. ΔNODR (**D**). For all the blots equal loading of protein was ensured with ß-actin. Representative blots are shown, a total of at least 3 independent experiments were performed. Statistical analysis was performed using a one way-ANOVA with Fisher's LSD test, VCAM-1 inhibition - TNFα versus treatment, HO-1 induction medium versus treatment (n.s. non-significant, * $p < 0.05$, ** $p < 0.001$, ***$p<0.0001$).

**Figure 1:**

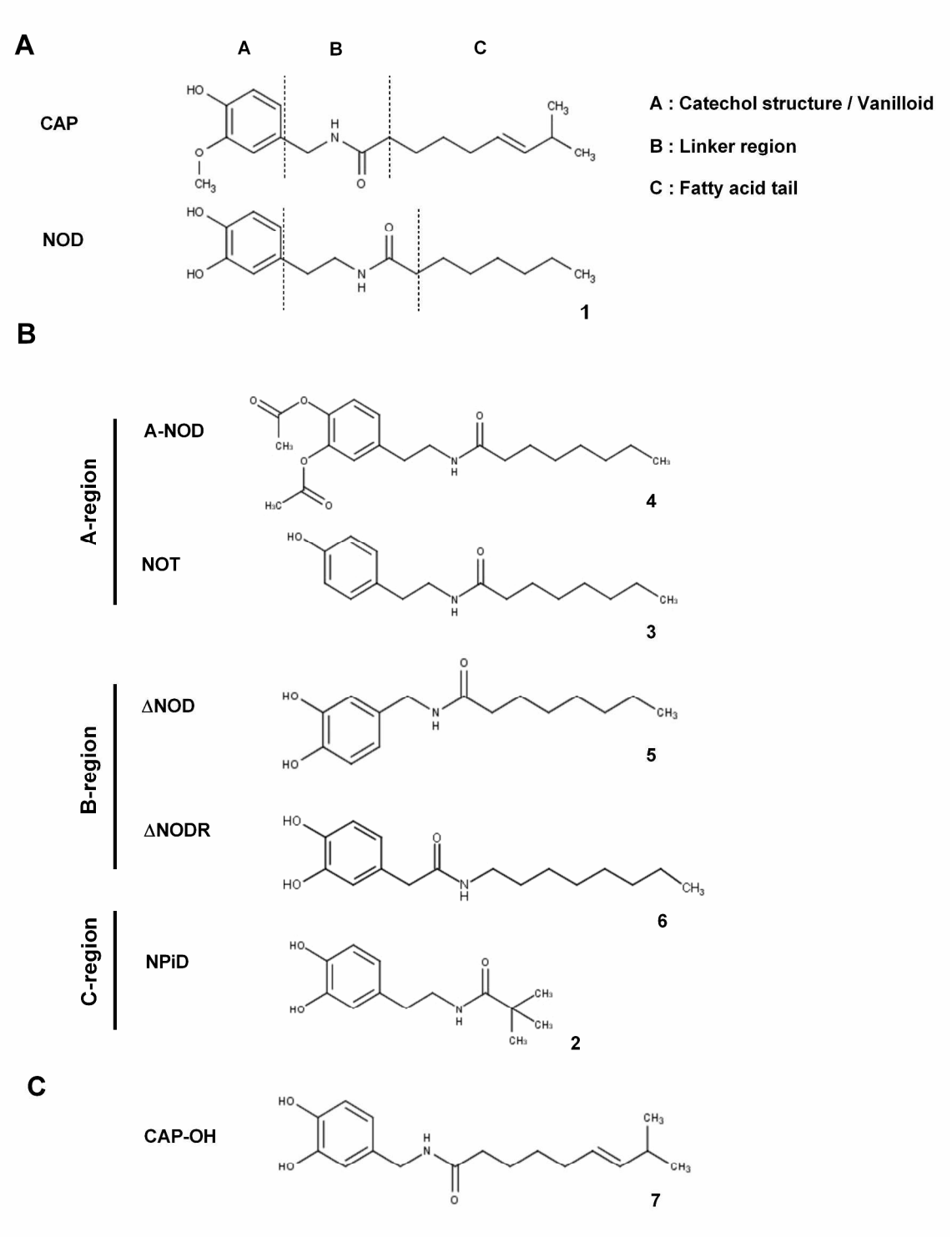
A
A
B
C
CAP
NOD
A : Catechol structure / Vanilloid
B : Linker region
C : Fatty acid tail
1
B
A-region
A-NOD
NOT
4
3
B-region
ΔNOD
ΔNODR
5
6
C-region
NPiD
2
C
CAP-OH
7

**Figure 2:**

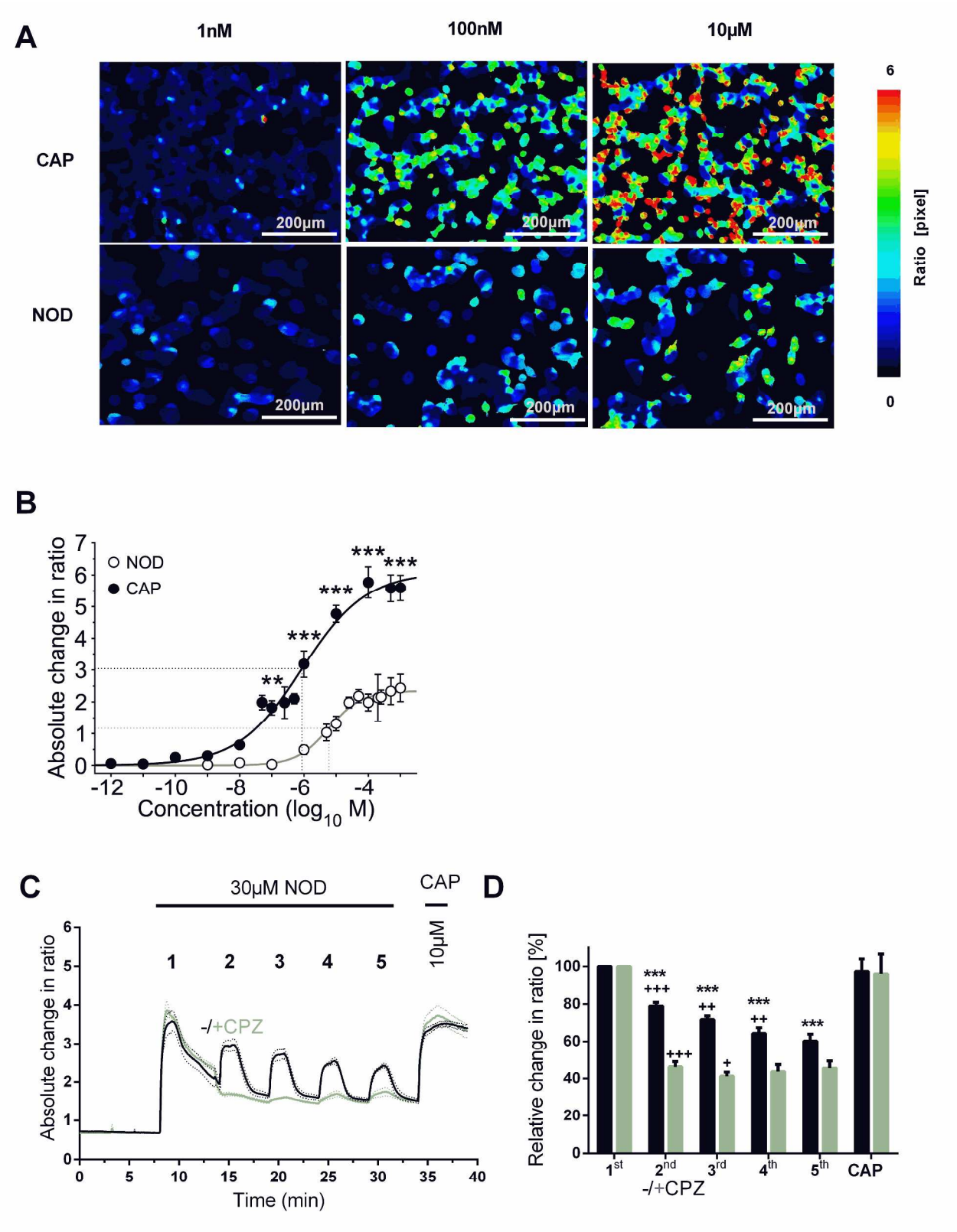
A
1nM
100nM
10µM
CAP
NOD
200µm
6
0
Ratio [pixel]
B
NOD
CAP
Absolute change in ratio
Concentration (log10 M)
C
30µM NOD
CAP
10µM
1
2
3
4
5
-/+CPZ
Absolute change in ratio
Time (min)
D
Relative change in ratio [%]
1st
2nd
3rd
4th
5th
CAP
-/+CPZ

**Figure 3:**

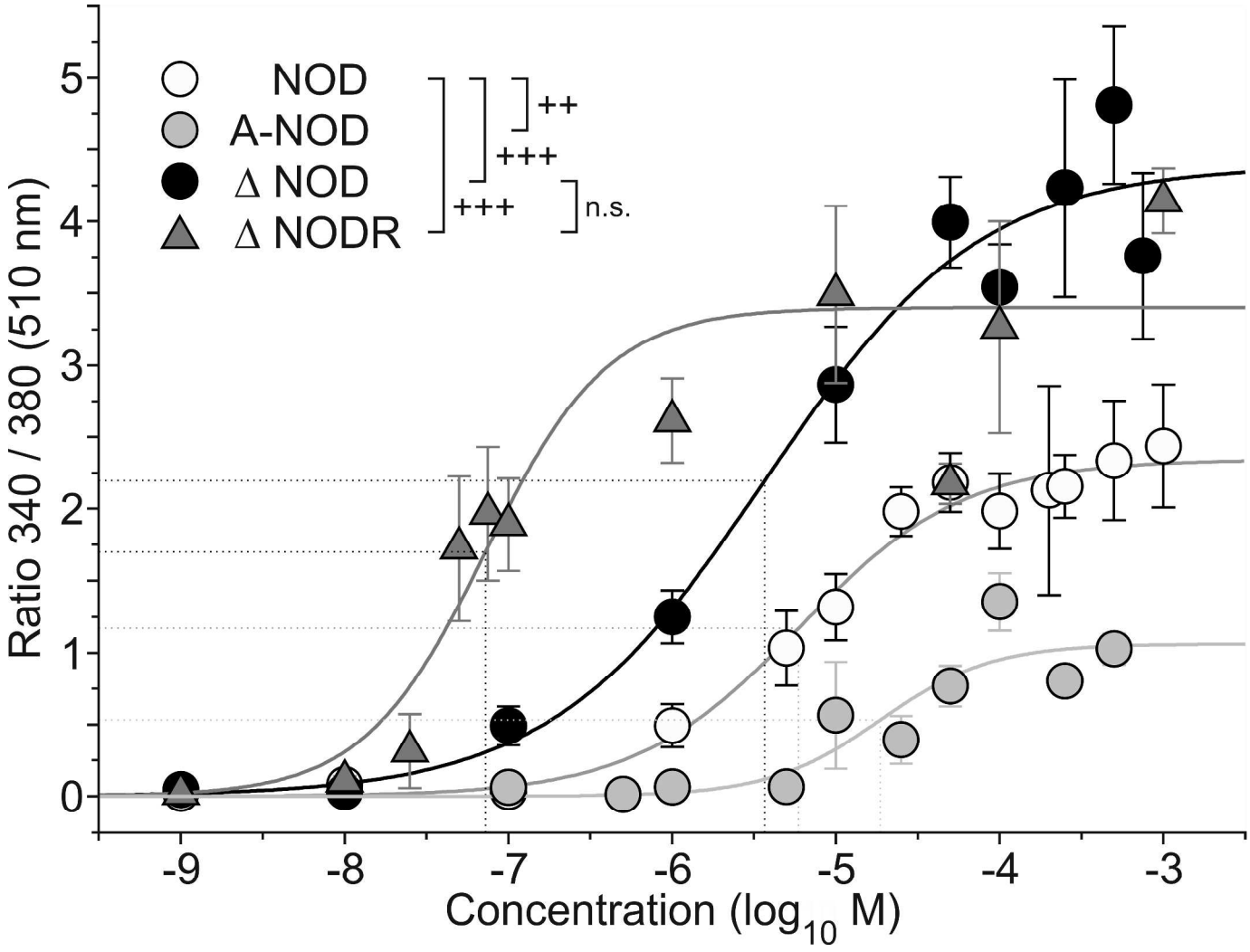
NOD
A-NOD
Δ NOD
Δ NODR
++
+++
+++
n.s.
Ratio 340 / 380 (510 nm)
Concentration (log10 M)
0
1
2
3
4
5
-9
-8
-7
-6
-5
-4
-3

**Figure 4**

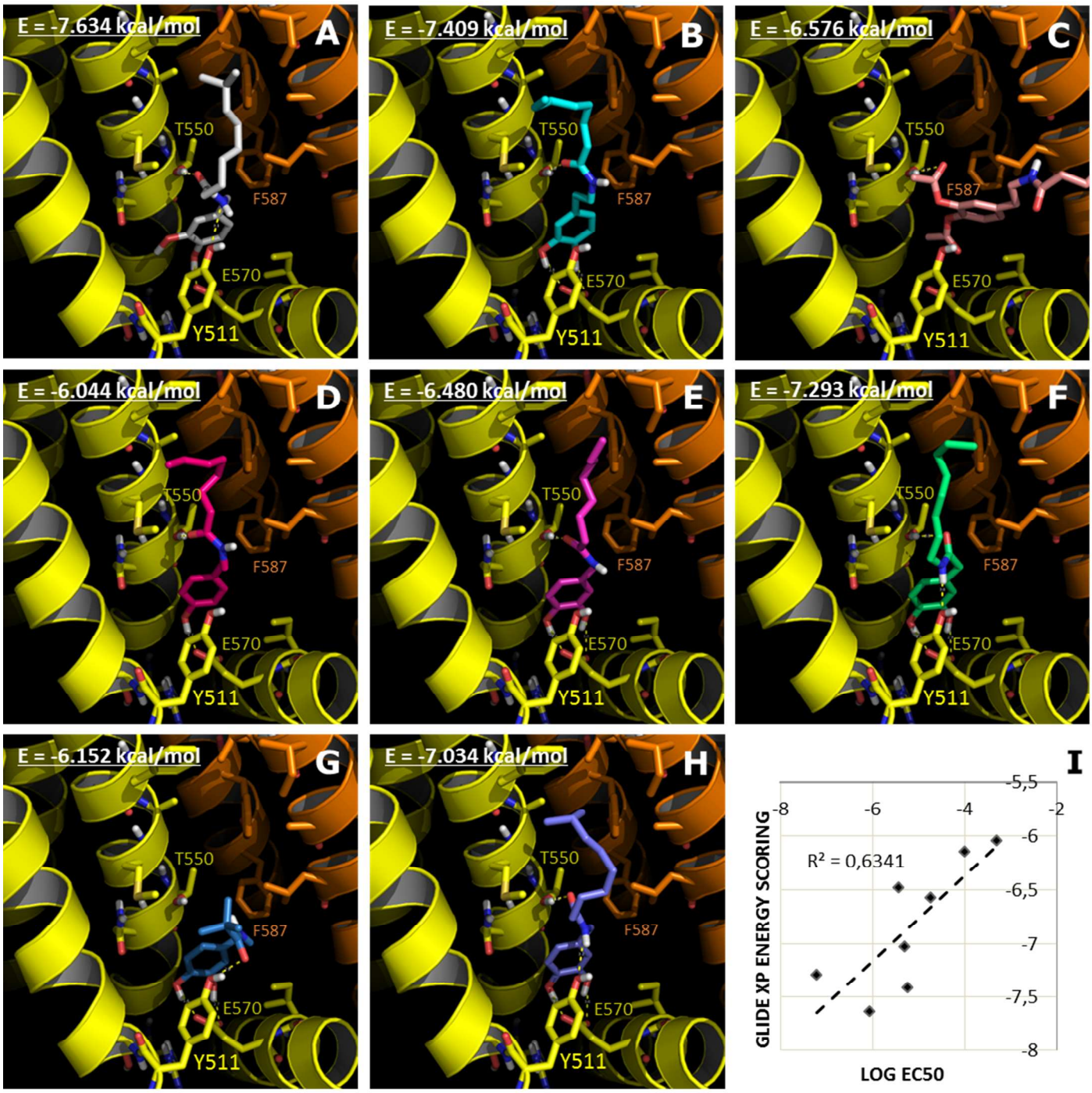
E = -7.634 kcal/mol
A
T550
F587
E570
Y511
E = -7.409 kcal/mol
B
T550
F587
E570
Y511
E = -6.576 kcal/mol
C
T550
F587
E570
Y511
E = -6.044 kcal/mol
D
T550
F587
E570
Y511
E = -6.480 kcal/mol
E
T550
F587
E570
Y511
E = -7.293 kcal/mol
F
T550
F587
E570
Y511
E = -6.152 kcal/mol
G
T550
F587
E570
Y511
E = -7.034 kcal/mol
H
T550
F587
E570
Y511
I
R² = 0,6341
GLIDE XP ENERGY SCORING
LOG EC50
-5,5
-6
-6,5
-7
-7,5
-8
-8
-6
-4
-2

**Figure 5**

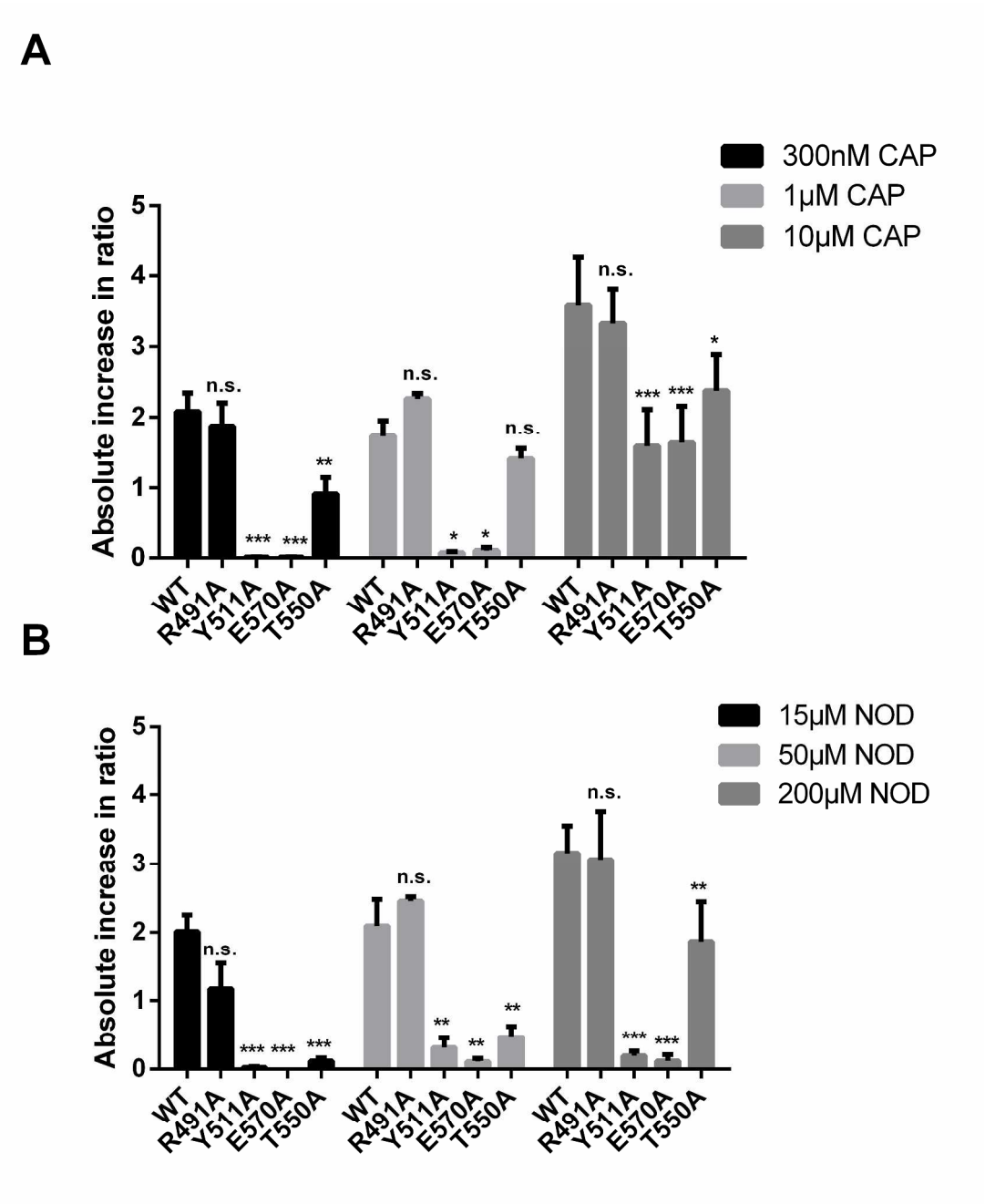
A
300nM CAP
1μM CAP
10μM CAP
Absolute increase in ratio
0
1
2
3
4
5
n.s.
n.s.
n.s.
n.s.
*
**
***
WT
R491A
Y511A
E570A
T550A
B
15μM NOD
50μM NOD
200μM NOD
Absolute increase in ratio
n.s.
n.s.
n.s.
**
***

**Figure 6**

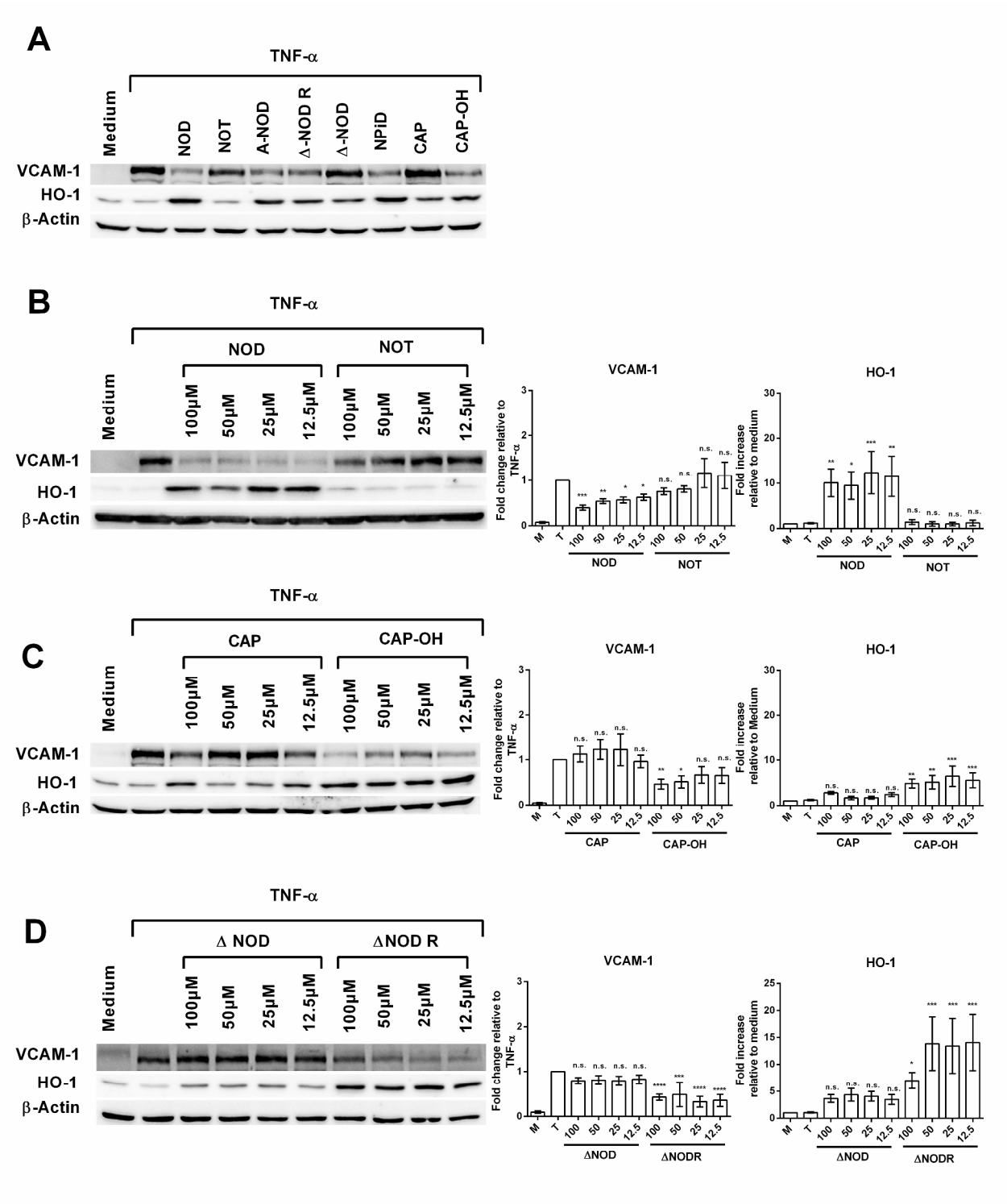
A
TNF-α
Medium
NOD
NOT
A-NOD
Δ-NOD R
Δ-NOD
NPiD
CAP
CAP-OH
VCAM-1
HO-1
β-Actin
B
TNF-α
NOD
NOT
100μM
50μM
25μM
12.5μM
VCAM-1
HO-1
β-Actin
Fold change relative to TNF-α
Fold increase relative to medium
C
TNF-α
CAP
CAP-OH
Fold increase relative to Medium
D
TNF-α
Δ NOD
ΔNOD R
ΔNOD
ΔNODR

## Table of graphics